Short-wavelength upconversion emissions in Ho^{3+}/Yb^{3+} codoped glass ceramic and the optical thermometry behavior

Wei Xu,[1] Xiaoyang Gao,[2] Longjiang Zheng,[2] Zhiguo Zhang,[1,3,*] and Wenwu Cao [1,4,5]

[1] *Condensed Mater Science and Technology, Harbin Institute of Technology, Harbin 150001, China*
[2] *Institute of electrical engineering, Yanshan University, Qinhuangdao, 066004, China*
[3] *Laboratory of Sono- and photo-theranostic Technologies, Harbin Institute of Technology, Harbin 150001, China*
[4] *Materials Research Institute, The Pennsylvania State University, Pennsylvania 16802, USA*
[5] *dzk@psu.edu*
* *zhangzhiguo@hit.edu.cn*

Abstract: Ho^{3+}/Yb^{3+} codoped glass ceramic was prepared by melt-quenching and subsequent thermal treatment. Under a 980 nm diode laser excitation, upconversion emissions from Ho^{3+} ions centered at 540, 650, and 750 nm were greatly enhanced compared with those in the precursor glass. Especially, the short-wavelength upconversion emissions centered at 360, 385, 418, 445, and 485 nm were successfully obtained in the glass ceramic. An explanation for this phenomenon is given based on the fluorescence decay curve measurements. In addition, an optical temperature sensor based on the blue upconversion emissions from $^5F_{2,3}/^3K_8 \rightarrow {}^5I_8$ and $^5F_1/^5G_6 \rightarrow {}^5I_8$ transitions in Ho^{3+}/Yb^{3+} codoped glass ceramic has been developed. It was found that by using fluorescence intensity ratio technique, appreciable sensitivity for temperature measurement can be achieved by using the Ho^{3+}/Yb^{3+} codoped glass ceramic. This result makes the Ho^{3+}/Yb^{3+} codoped glass ceramic be a promising candidate for sensitive optical temperature sensor with high resolution and good accuracy.

OCIS codes: (190.7220) Upconversion; (160.4760) Optical properties; (300.2140) Emission; (280.4788) Optical sensing and sensors.

References and links

1. F. Auzel, "Upconversion and anti-stokes processes with f and d ions in solids," Chem. Rev. **104**(1), 139–174 (2004).
2. E. Downing, L. Hesselink, J. Ralston, and R. Macfarlane, "A three-color, solid-state, three-dimensional display," Science **273**(5279), 1185–1189 (1996).
3. S. Sivakumar, F. C. J. M. van Veggel, and P. S. May, "Near-infrared (NIR) to red and green up-conversion emission from silica sol-gel thin films made with La0.45Yb0.50Er0.05F_3 nanoparticles, hetero-looping-enhanced energy transfer (Hetero-LEET): a new up-conversion process," J. Am. Chem. Soc. **129**(3), 620–625 (2007).
4. A. Patra, C. S. Friend, R. Kapoor, and P. N. Prasad, "Upconversion in Er^{3+}: ZrO_2 nanocrystals," J. Phys. Chem. B **106**(8), 1909–1912 (2002).
5. J. A. Capobianco, J. C. Boyer, F. Vetrone, A. Speghini, and M. Bettinelli, "Optical spectroscopy and upconversion studies of Ho^{3+}-doped bulk and nanocrystalline Y_2O_3," Chem. Mater. **14**(7), 2915–2921 (2002).
6. Y. Guyot, R. Moncorge, L. F. Merkle, A. Pinto, B. Mclntosh, and H. Verdun, "Luminescence properties of Y_2O_3 single crystals doped with Pr^{3+} or Tm^{3+} and codoped with Yb^{3+}, Tb^{3+} or Ho^{3+} ions," Opt. Mater. **5**(1-2), 127–136 (1996).
7. X. Wang, Y. Bu, S. Xiao, X. Yang, and J. W. Ding, "Upconversion in Ho^{3+}-doped YbF_3 particle prepared by coprecipation method," Appl. Phys. B **93**(4), 801–807 (2008).
8. G. Y. Chen, G. H. Yang, B. Aghahadi, H. J. Liang, Y. Liu, L. Li, and Z. G. Zhang, "Ultraviolet-blue upconversion emissions of Ho^{3+} ions," J. Opt. Soc. Am. B **27**(6), 1158–1164 (2010).
9. J. F. Suyer, A. Aebischer, D. Biner, P. Gerner, J. Grimm, S. Heer, K. W. Krämer, C. Reinhard, and H. U. Güdel, "Novel materials doped with trivalent lanthanides and transition metal ions showing near-infrared to visible photon upconversion," Opt. Mater. **27**(6), 1111–1130 (2005).
10. F. Lahoz, I. R. Martín, and A. Briones, "Infrared-laser induced photon avalanche upconversion in Ho^{3+}–Yb^{3+} codoped fluoroindate glasses," J. Appl. Phys. **95**(6), 2957–2962 (2004).
11. G. J. Ding, F. Gao, G. H. Wu, and D. H. Bao, "Bright up-conversion green photoluminescence in Ho^{3+}-Yb^{3+} co-doped $Bi_4Ti_3O_{12}$ ferroelectric thin films," J. Appl. Phys. **109**(12), 123101 (2011).

#168888 - $15.00 USD Received 22 May 2012; revised 4 Jul 2012; accepted 4 Jul 2012; published 23 Jul 2012

12. F. Lahoz, I. R. Martín, and J. M. Calvilla-Quintero, "Ultraviolet and white phonon avalanche upconversion in Ho^{3+} doped nanophase glass ceramic," Appl. Phys. Lett. **86**(5), 051106 (2005).
13. D. Q. Chen, Y. S. Wang, Y. L. Yu, and P. Huang, "Intense ultraviolet upconversion luminescence from Tm^{3+}/Yb^{3+}:beta-YF_3 nanocrystals embedded glass ceramic," Appl. Phys. Lett. **91**(5), 051920 (2007).
14. S. Tanabe, H. Hayashi, T. Hanada, and N. Onodera, "Fluorescence properties of Er^{3+} ions in glass ceramics containing LaF_3 nanocrystals," Opt. Mater. **19**(3), 343–349 (2002).
15. Y. Kawamoto, R. Kanno, and J. Qiu, "Upconversion luminescence of Er^{3+} in transparent SiO_2-PbF_2-ErF_3 glass ceramic," J. Mater. Sci. **33**(1), 63–67 (1998).
16. B. N. Samson, P. A. Tick, and N. F. Borrelli, "Efficient neodymium-doped glass-ceramic fiber laser and amplifier," Opt. Lett. **26**(3), 145–147 (2001).
17. M. Pollnau, P. J. Hardman, M. A. Kern, W. A. Clarkson, and D. C. Hanna, "Upconversion-induced heat generation and thermal lensing in Nd: YLF and Nd: YAG," Appl. Phys. Lett. **58**, 16076–16092 (1998).
18. K. Y. Wu, J. B. Cui, X. X. Kong, and Y. J. Wang, "Temperature dependent upconversion luminescence of Yb/Er codoped $NaYF_4$ nanocrystals," J. Appl. Phys. **110**(5), 053510 (2011).
19. H. Berthou and C. K. Jörgensen, "Optical-fiber temperature sensor based on upconversion-excited fluorescence," Opt. Lett. **15**(19), 1100–1102 (1990).
20. S. A. Wade, S. F. Collins, and G. W. Baxter, "Fluorescence intensity ratio technique for optical fiber point temperature sensing," J. Appl. Phys. **94**(8), 4743–4756 (2003).
21. V. K. Rai, "Temperature sensor and optical sensors," Appl. Phys. B **88**(2), 297–303 (2007).
22. V. Lavín, F. Lahoz, I. R. Martín, U. R. Rodríguze-Mendoza, and J. M. Cáceres, "Infrared-to-visible photon avalanche upconversion dynamics in Ho^{3+}-doped fluorozirconate glasses at room temperature," Opt. Mater. **27**(11), 1754–1761 (2005).
23. L. Gomes, L. C. Courrol, L. V. G. Tarelho, and I. M. Ranieri, "Cross-relaxation process between +3 rare-earth ions in $LiYF_4$ crystals," Phys. Rev. B Condens. Matter **54**(6), 3825–3829 (1996).
24. S. Tanabe, S. Yoshii, K. Hirao, and N. Soga, "Upconversion properties, multiphonon relaxation, and local environment of rare earth ions in fluorophosphates glasses," Phys. Rev. **45**(9), 4620–4625 (1992).
25. F. Lahoz, I. R. Matín, and J. Méndez-Ramos, "Dopant distribution in a Tm^{3+}-Yb^{3+} codoped silica based glass ceramic: an infrared-laser induced upconversion study," J. Appl. Phys. **120**, 6180–6190 (2004).
26. D. L. Dexter, "A theory of sensitized luminescence in solids," J. Chem. Phys. **21**(5), 836–850 (1953).
27. S. A. Wade, S. F. Collins, G. W. Baxter, and G. Monnom, "Effect of strain on temperature measurements using the fluorescence intensity ratio technique (with Nd^{3+} and Yb^{3+} doped silica fibers)," Rev. Sci. Instrum. **72**(8), 3180–3185 (2001).
28. P. V. dos Santos, M. T. de Araujo, A. S. Gouveia-Neto, J. A. Medeiros Neto, and A. S. B. Sombra, "Optical temperature sensing using upconversion fluorescence emission in Er^{3+}/Yb^{3+} codoped chalcogenide glass," Appl. Phys. Lett. **73**(5), 578–580 (1998).
29. P. Haro-González, I. R. Martín, L. L. Martín, F. S. León-Luis, C. Pérez-Rodríguez, and V. Lavín, "Characterization of Er^{3+} and Nd^{3+} doped strontium Barium Niobate glass ceramic as temperature sensors," Opt. Mater. **33**(5), 742–745 (2011).
30. V. K. Rai, D. K. Rai, and S. B. Rai, "Pr^{3+} doped lithium tellurite glass as a temperature sensor," Sen. Actuators A **128**(1), 14–17 (2006).
31. S. A. Wade, J. C. Muscat, S. F. Collins, and G. W. Baxter, "Nd^{3+} doped optical temperature sensor using the fluorescence intensity ratio technique," Rev. Sci. Instrum. **70**(11), 4279–4282 (1999).
32. E. Maurice, S. A. Wade, S. F. Collins, G. Monnom, and G. W. Baxter, "Self-referenced point temperature sensor based on a fluorescence intensity ratio in Yb^{3+} doped silica fiber," Appl. Opt. **36**(31), 8264–8269 (1997).
33. B. S. Cao, Y. Y. He, Z. Q. Feng, Y. S. Li, and B. Dong, "Optical temperature sensing behavior of enhanced green upconversion emissions from Er^{3+}-Mo:$Yb_2Ti_2O_7$ nanophosphor," Sen. Actuators B **159**(1), 8–11 (2011).
34. S. F. León-Luis, U. R. Rodríguez-Mendoza, E. Lalla, and V. Lavín, "Temperature sensor based on the Er^{3+} green upconverted emission in a fluorotellurite glass," Sen. Actuators B **158**(1), 208–213 (2011).
35. R. K. Verma and S. B. Rai, "Laser induced optical heating from Yb^{3+}/Ho^{3+}: $Ca_{12}Al_{14}O_{33}$ and its applicability as a thermal probe," J. Quant. Spectrosc. Radiat. Transf. **113**(12), 1594–1600 (2012).

1. Introduction

In recent years, the study on the upconversion (UC) materials have attracted considerable attention because of their wide applications such as color displays, short-wavelength lasers, IR quantum counter detectors, optical sensing, optical communications, and biomedical diagnostics [1, 2]. UC, i.e., photoexcitation at a long wavelength followed by luminescence at a shorter wavelength, is typically observed in compounds containing rare earth (RE) ions. The unique optical properties for RE ions arise from the weak interaction of the 4*f* elections with the ligand field due to the shielding effect of the outer 5*s* and 5*p* orbitals, which results in sharp intra-4*f* transitions. In addition, the RE ions possess abundant electronic states at various energies, which afford them the ability to absorb one or more low-energy near infrared (NIR) photons and subsequently convert them to high-energy emissions [3]. Thus, the generation of UC fluorescence can be easily realized by ample availability of well-matching, cost-effective, and high-power near infrared diode lasers. Many RE ions, including Er^{3+}, Ho^{3+}, Tm^{3+}, and

#168888 - $15.00 USD Received 22 May 2012; revised 4 Jul 2012; accepted 4 Jul 2012; published 23 Jul 2012

Pr^{3+}, have been extensively reported for their UC luminescence [4–8]. However, short-wavelength UC emissions (from ultraviolet to blue) from RE ions, especially from Ho^{3+}, induced by NIR lasers have rarely been investigated presently.

It is well known that Ho^{3+} has abundant energy levels in the spectroscopic range of ultraviolet to NIR [1]. Although the short-wavelength UC emissions of Ho^{3+} was reported in Ho^{3+} doped $LiYF_4$ and YF_3 via synchrotron radiation, these emissions induced by NIR laser excitation are not observed [9]. And it is known that Ho^{3+} sensitized by Yb^{3+} not only can generate strong visible UC emissions, but also can result in visible photon avalanche UC emissions under NIR laser excitation [10]. Green and red UC emissions from Ho^{3+}/Yb^{3+} codoped materials under 980 nm laser excitation have been widely studied, and photon avalanche for visible UC emissions in Ho^{3+} doped or Ho^{3+}/Yb^{3+} codoped materials have also been studied under 750 or 840 nm excitations [10, 11], but the short-wavelength emissions are scarcely observed. So far, just very a few works have obtained the UC emissions of Ho^{3+} ions in the ultraviolet-blue spectral range excited by NIR laser [7, 8, 12]. However, the weak chemical and physical stability of the fluoride hosts significantly limits their practical applications [7, 8]. It, therefore, is of great scientific interest and importance to obtain the short-wavelength UC emissions of Ho^{3+} ions in an appropriate host matrix.

As is well known, the oxyfluoride glass ceramic has been proven to be one of the most promising luminescent materials for its advantages combined with low phonon energy for fluorides and desirable mechanical and chemical performances for oxides [13, 14]. This kind of material is generally fabricated through controlling crystallization of the defined fluoride nanophase from the precursor glass by thermal treatment. And by incorporating abundant RE ions into the fluoride nanocrystals, efficient UC emissions are readily obtained [15]. In addition, the suitability of the oxyfluoride glass ceramic to be fibered has been demonstrated [16]. This characteristic makes this kind material compatible with a range of optical schemes and highlights the potential applications on optical amplifiers and laser systems.

Meanwhile, due to the strong dependence of transitions from the elections in 4*f* systems of RE ions on the temperature conditions [17, 18], the thermal behavior of UC fluorescence becomes increasingly important for further understanding the UC mechanisms in general and finding the potential uses, especially, on the optical thermal sensing [19–21]. Thus, in the present work, we synthesized Ho^{3+}/Yb^{3+} codoped oxyfluoride glass ceramic through high temperature solid-state reaction and the subsequent thermal treatment. Under a 980 nm diode laser excitation, the UC emissions in the ultraviolet-blue range were successfully obtained in the glass ceramic. Analysis based on the luminescence decay curves was performed to explain this phenomenon. In addition, the temperature dependent blue emissions from Ho^{3+}/Yb^{3+} codoped glass ceramic were investigated at temperatures ranging from 303 to 643 K. A much higher sensitivity for temperature measurement was achieved here.

2. Experimental

The glass ceramic is prepared with the following starting composition ratios (in mol %): $50SiO_2$-$50PbF_2$-$0.05Ho_2O_3$-$0.5Yb_2O_3$. The fully mixed chemicals are melted in a covered alumina crucible at 1000 °C for 1 hour in a SiC-resistance electric furnace in air. Then, the melt is cast into a preheated stainless steel mold and naturally cooled down to room temperature to form the precursor glass. The precursor glass is heated to 460 °C with a heating rate of 10 K/min, and then hold for 3 hours to form transparent glass ceramic through crystallization. The resulting samples are cut and polished into the size of 10 mm × 8 mm × 2 mm for optical measurements.

Differential thermal analysis (DTA) measurement was carried out by the differential thermal analyzer (Rigaku TG-DTA TG8120) to confirm the glass transition temperature (T_g) and the crystallization peak temperature (T_c). X-ray diffraction (XRD) patterns were acquired using a Rigaku D/max-γB diffractometer with Cu Kα radiation (λ = 0.15418 nm). The UC luminescence spectra were recorded by Zolix-SBP300 grating spectrometer equipped with a CR131 photomultiplier tube. A 980 nm diode laser is used as the pump source. The luminescence decay curves are measured by the 980 nm diode laser modulated through

#168888 - $15.00 USD Received 22 May 2012; revised 4 Jul 2012; accepted 4 Jul 2012; published 23 Jul 2012

square-wave electric current and recorded by Tektronix DPO 4140 oscilloscope. When measuring the luminescence decay curves for the infrared emissions, the light signal was detected by InGaAs photodiode. To investigate the temperature dependent UC luminescence, the sample was placed in a mini furnace and its temperature was increased from 303 to 643 K. The temperature of sample was monitored by a copper-constantan thermocouple and controlled by a proportional-integral-derivative loop feedback temperature control system.

To investigate the temperature dependent UC luminescence, the sample was put into a quartz tube and then placed in a home-made mini Si-C furnace. The sample was heated from 303 to 643 K and the temperature of sample was monitored by a copper-constantan thermocouple with an accuracy of ± 1.5 K and controlled by a proportional-integral-derivative loop feedback temperature control system. The UC luminescence signal of the sample generated by the excitation of 980 nm laser was finally coupled into the grating spectrometer through a quartz lens.

3. Results

3.1. Upconversion emissions

Figure 1 shows the DTA curve of the glass. It can be observed that the glass transition occurred at around 409 °C and distinct crystallization peak began at 450 °C, centered at 489 °C and ended at 539 °C. It was found that the glass heated at 489 °C lost easily its transparency. To get transparent glass ceramic, the heat treatment temperature was selected to be 460 °C based on the experiment experience. The XRD patterns of the glass and the glass ceramic are shown in Fig. 2. There are only two humps in the XRD curve for the glass, indicating its amorphous structure. However, after thermal treatment, intense diffraction peaks attributed to β-PbF_2 nanocrystals [15] emerge in the XRD patterns, reflecting the crystallization during thermal treatment.

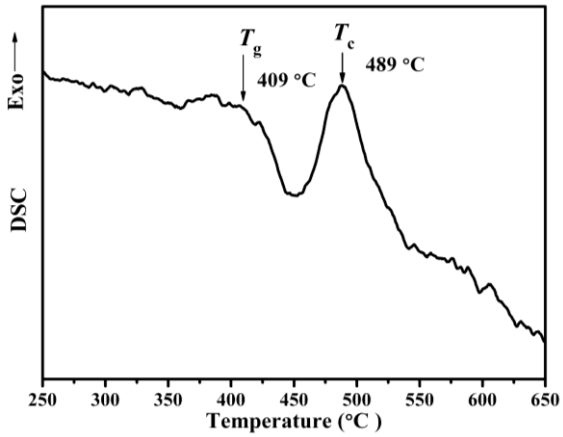

Fig. 1. DTA curve for the SiO_2-PbF_2-Ho_2O_3-Yb_2O_3 glass.

#168888 - $15.00 USD Received 22 May 2012; revised 4 Jul 2012; accepted 4 Jul 2012; published 23 Jul 2012

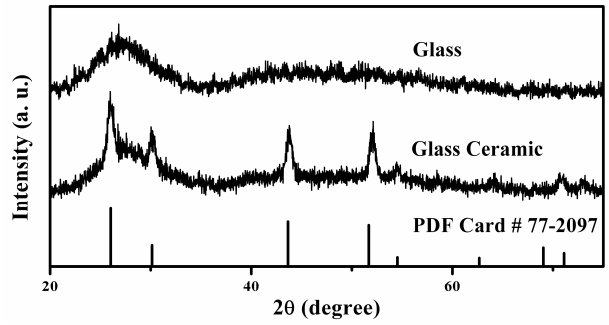

Fig. 2. XRD patterns for Ho^{3+}/Yb^{3+} codoped glass and glass ceramic.

Figure 3 shows the room temperature UC emission spectra for the Ho^{3+}/Yb^{3+} codoped precursor glass and glass ceramic under 980 nm excitation with the pumping power of 650 mW. Both spectra exhibit green, red, and NIR emissions bands of Ho^{3+} ions originated from the following three transitions: $^5S_2/^5F_4 \rightarrow {}^5I_8$(~540 nm), $^5F_5 \rightarrow {}^5I_8$(~650 nm), and $^5S_2/^5F_4 \rightarrow {}^5I_7$(~750 nm). In comparison with the precursor glass, the intensity for these UC emissions in the glass ceramic is greatly enhanced, and the green, red, and NIR emissions are respectively enhanced to be about 26, 20, and 5 times. Especially, the short-wavelength UC emissions ranging from ultraviolet to blue centered around 362 nm, 390 nm, 420 nm, 445 nm, and 485 nm, which are not detected in the precursor glass, are successfully obtained in the glass ceramic. Such emissions can be assigned to the transitions from $^5F_2$, $_3/^3K_8$, $^5F_1/^5G_6$, $^5G_5$, $^5G_4/^3K_7$, and $^5G_5/^3H_6$ of Ho^{3+} to the ground state $^5I_8$, respectively [7, 8]. In addition, the UC emission bands in the glass ceramic exhibit obvious Stark splits, which indicates the successful incorporation of RE ions into the β-PbF_2 nanocrystals after thermal treatment.

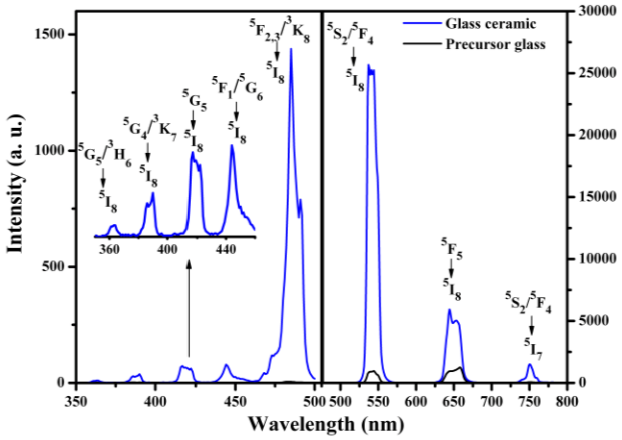

Fig. 3. Upconversion emissions for the Ho^{3+}/Yb^{3+} codoped precursor glass and glass ceramic

3.2. Upconversion mechanisms

To understand the UC mechanisms, the pump power dependences of emissions for the glass ceramic were investigated. It is known that at the unsaturation condition, the UC emission intensity (I_{UP}) depends on the excitation power (P) and follows the below relationship

$$I_{UP} \propto P^n, \quad (1)$$

#168888 - $15.00 USD Received 22 May 2012; revised 4 Jul 2012; accepted 4 Jul 2012; published 23 Jul 2012

where n is the number of the pumping photons required to excite RE ions from the ground state to the emitting excited state. The power dependence for the UC emissions in the glass ceramic is shown in Fig. 4 by a log-log plot. As illustrated in Fig. 4(a), slope n values of the linear fittings are 1.34, 1.51, and 1.28 for the green, red, and NIR UC emissions, respectively. The n values suggest two-photon process for these UC emissions. Meanwhile, as illustrated in Fig. 4(b), the slopes of the linear fitting are 2.28 for $^5F_{2,3}/^3K_8 \rightarrow {}^5I_8$, 2.45 for $^5F_1/^5G_6 \rightarrow {}^5I_8$, 2.42 for $^5G_5 \rightarrow {}^5I_8$, 2.63 for $^5G_4/^3K_7 \rightarrow {}^5I_8$, and 2.66 for $^5G_5/^3H_6 \rightarrow {}^5I_8$ transition, indicating three pumping photons are required to populate the $^5F_{2,3}/^3K_8$, $^5F_1/^5G_6$, $^5G_5$, $^5G_4/^3K_7$, and $^5G_5/^3H_6$ levels. Figure 5 shows the energy level diagrams of Ho^{3+} and Yb^{3+} ions, as well as the proposed mechanisms to explain the short-wavelength UC emissions. The pumping photons of 980 nm can be efficiently absorbed by Yb^{3+} ions, and the $^5S_2/^5F_4$ and $^5F_5$ energy levels can be populated through two successive energy transfers from Yb^{3+} to Ho^{3+} ions. Subsequently, one energy transfer from excited Yb^{3+} can promote the Ho^{3+} ions on the $^5S_2/^5F_4$ or $^5F_5$ onto the $^5G_5/^3H_6$ or $^5G_4/^3K_7$ states. Alternatively, the $^5G_4/^3K_7$ levels can be populated via the multiphonon nonradiative relaxation from $^5G_5/^3H_6$. Then, the $^5F_{2,3}/^3K_8$, $^5F_1/^5G_6$, and $^5G_5$ levels are populated by the multiphonon nonradiative relaxations from their upper levels. In addition, some possible cross-relaxation (CR) processes may also occurs [22, 23], as illustrated in Fig. 5.

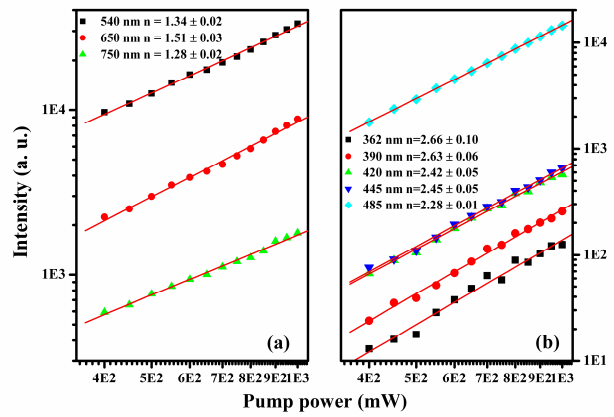

Fig. 4. Log-log plot of the upconversion emission intensity versus the pumping power.

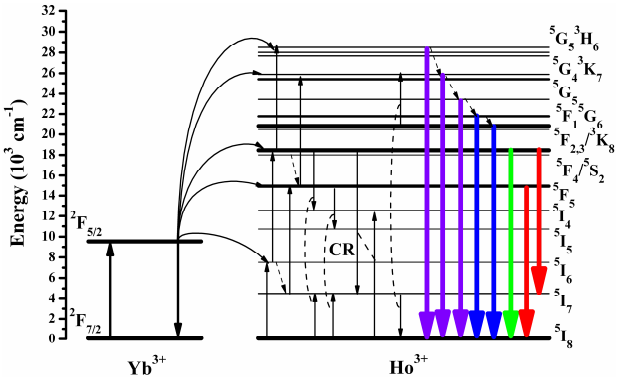

Fig. 5. Energy level diagram of Yb^{3+} and Ho^{3+} ions as well as the proposed upconversion mechanisms.

#168888 - $15.00 USD Received 22 May 2012; revised 4 Jul 2012; accepted 4 Jul 2012; published 23 Jul 2012

3.3. Analysis of the luminescence decay curves

Note that the green, red, and NIR UC emissions of Ho^{3+} ions were enhanced dramatically after thermal treatment on the precursor glass, and the short wavelength emissions from ultraviolet to blue were successfully obtained in the glass ceramic. As is well known, a significant factor affecting the UC efficiency of RE ions is the multiphonon nonradiative relaxation rate W_{NR}, which follows the below equation [24]

$$W_{NR} \propto \left[1-\exp\left(-\hbar w / k_B T\right)\right]^{-P}, \tag{2}$$

where $\hbar w$ is the phonon energy in the surrounding medium; k_B is Boltzmann constant, and T is the absolute temperature; P is the number of phonons required to complement the energy gap ΔE between the upper and the lower levels, and P can be calculated according to

$$P = \Delta E / \hbar w, \tag{3}$$

Equations (2) and (3) suggest that medium with lower phonon energy results in a smaller multiphonon nonradiative relaxation rate and consequently improves the luminescence efficiency.

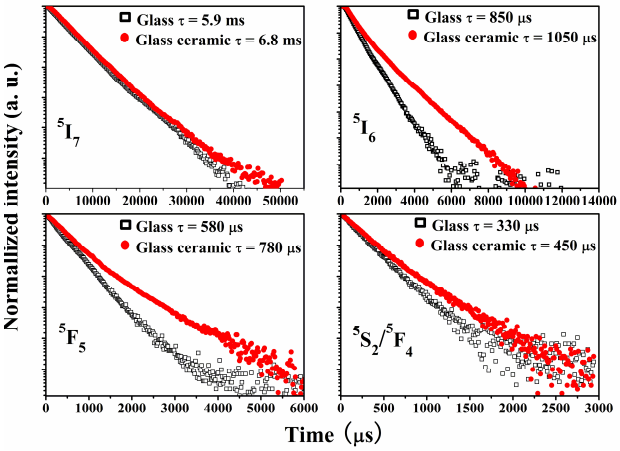

Fig. 6. Luminescence decay curves for the energy levels of Ho^{3+} ions in the glass and the glass ceramic.

Figure 6 shows the luminescence decay curves for $^5I_7$, $^5I_6$, $^5F_5$, and $^5S_2/^5F_4$ states in the glass and the glass ceramic. It is observed that the lifetimes for these states are increased in the glass ceramic compared with those in the precursor glass. This is mainly because that in the precursor glass, Ho^{3+} ions are coupled to the non-bridging oxygen on the strong O-Si bonds with the phonon mode around 930 cm^{-1} [15]; in the glass ceramic, most of RE ions are incorporated into the fluoride nanocrystals [25]. In such a case, Ho^{3+} ions are shielded from the direct coupling with the nonbridging oxygen of O-Si and coupled to a weaker phonon mode of 230 cm^{-1} for Pb-F [15]. The lower phonon energy environment of the fluoride nanocrystals can weaken the multiphonon nonradiative relaxations and contribute to the UC emissions of Ho^{3+} ions in the glass ceramic. As the intermediate states, the longer lifetimes for $^5S_2/^5F_4$ and $^5F_5$ states also contribute to the population of the higher energy levels. Due to the undetected ultraviolet-blue short wavelength UC emission signals in the precursor glass, the comparison between the lifetimes for the upper energy levels of Ho^{3+} ions in the precursor glass and the glass ceramic are not performed. However, longer luminescence lifetimes for $^5F_{2,\,3}/^3K_8$, $^5F_1/^5G_6$, $^5G_5$, $^5G_4/^3K_7$, and $^5G_5/^3H_6$ states in the glass ceramic can also be expected.

In addition, according to the Dexter theory [26], the energy transfer rate between the RE ions is proportional to R^{-6}, where R is the distance between a sensitizer and an acceptor. Since

#168888 - $15.00 USD Received 22 May 2012; revised 4 Jul 2012; accepted 4 Jul 2012; published 23 Jul 2012

most of Ho^{3+} and Yb^{3+} ions are concentrated into β-PbF_2 nanocrystals in the glass ceramic, the distance between Ho^{3+} and Yb^{3+} ions becomes much shorter than that in the precursor glass. As a result, the energy transfer rate from Yb^{3+} to Ho^{3+} ions will be enhanced. The energy transfer rate $W_{Yb\rightarrow Ho}$ from Yb^{3+} to Ho^{3+} can be estimated from the following relation

$$W_{Yb\rightarrow Ho} = \frac{1}{\tau_{Yb-Ho}} - \frac{1}{\tau_{Yb}}. \quad (4)$$

The values of decay-time for Yb^{3+} in Ho^{3+}/Yb^{3+} codoped ($\tau_{Yb\text{-}Ho}$) and Yb^{3+} singly doped (τ_{Yb}) glass and glass ceramic are measured, respectively, and the $W_{Yb\rightarrow Ho}$ in the glass ceramic is estimated to be about 715 s^{-1}, which is much larger than that in the glass (~222 s^{-1}). The strengthened energy transfer from Yb^{3+} to Ho^{3+} ions also plays an important role in obtaining the short-wavelength UC emissions.

3.4. Optical thermometry based on the blue upconversion emissions of Ho^{3+} ions

Accurate and reliable measurement of temperature is a major requirement in the monitoring of changes in chemical, physical, and biological processes. Fluorescence temperature sensing technique has been attracted great interest for its high sensitivity and good accuracy [20]. Compared with the conventional technique, the fluorescence based sensors are especially advantages in the applications in the electromagnetically and/or thermally harsh environments, such as the electrical power station, oil refineries, coal mines, and building fire detection [27]. An optical temperature sensor is generally based on the fluorescence intensity ratio (FIR) technique, which is independent of signal losses and fluctuation in the excitation intensity and has the potential to further improve the measurement accuracy. Generally, the FIR utilizes the temperature dependent fluorescence from two thermally coupled energy levels of one type RE ions, and the energy gap ΔE between these two levels should be 200 $cm^{-1} \leq \Delta E \leq 2000$ cm^{-1}. As is known, the fluorescence of RE ions can be generated via UC and downconversion process by proper pumping source. But the former is more popular in the case of optical thermometry not only for the commercial excitation sources, but also for the eliminating of stray light which is easily introduced by downconversion excitation source. Till now, Er^{3+}, Pr^{3+}, Nd^{3+}, and Yb^{3+} have been developed as the activators for optical temperature sensors [20, 28–34].

For optical thermometry, it is of great importance to understand the rate at which the FIR changes for a change in temperature T. This value is known as the sensitivity. To allow the comparison between the sensitivities obtained from the FIR of different RE ions, the absolute sensitivity S is defined as [20, 21]

$$S \equiv \frac{\Delta E}{k_B T^2}. \quad (5)$$

Equation (5) suggests that using pairs of levels with larger energy difference are in favor of higher sensitivity. Currently, the largest sensitivity for optical temperature sensors based on the UC fluorescence is just limited in the materials with Nd^{3+} ions, the energy gap for the thermally coupled $^4F_{3/2}$ and $^4F_{5/2}$ levels being about 1000 cm^{-1} [31]. But to satisfy the thermometry requiring a higher sensitivity, the finding of the thermally coupled levels with much larger separation, from which luminescence can be easily produced via proper pumping, is becoming increasingly important.

From the emission spectra of Ho^{3+}/Yb^{3+} codoped glass ceramic, it is noted that the ΔE between $^5F_{2,3}/^3K_8$ and $^5F_1/^5G_6$ is about 1853 cm^{-1}, which satisfies the situation of thermally coupled levels and is much larger than that of Nd^{3+} ions. That is to say, the blue emissions from Ho^{3+}: $^5F_{2,3}/^3K_8$ and $^5F_1/^5G_6$ states can be utilized for optical thermometry with higher sensitivity [35]. To understand the characteristics for temperature sensing, the blue UC emissions from Ho^{3+}/Yb^{3+} codoped glass ceramic were studied as a function of temperature ranging from 303 to 643 K. Figure 7 shows the temperature dependent blue UC emissions for

#168888 - $15.00 USD Received 22 May 2012; revised 4 Jul 2012; accepted 4 Jul 2012; published 23 Jul 2012

Ho^{3+}/Yb^{3+} codoped glass ceramic. The pumping power of 980 nm laser is set as 650 mW. From Fig. 7, it can be seen that with the increase of temperature, the position for 485 nm fluorescence is not changed, but its intensity decreases gradually. In contrast, the intensity for $^5F_1/^5G_6 \rightarrow {}^5I_8$ transitions is slightly enhanced, and about 1.4 times enhancement is achieved at 583 K. In addition, the center wavelength for $^5F_1/^5G_6 \rightarrow {}^5I_8$ changes from 445 to 453 nm as temperature increases. Such phenomenon is interesting. This may be due to that the peak of the hypersensitive $^5I_8 \rightarrow {}^5G_6$ absorption band, which was measured to be around 453 nm at room temperature, exhibits blue-shift as temperature increases. In this case, the reabsorption effect could be weakened for the 453 nm emission but enhanced for the emission at 445 nm, so that the red-shift of the 440-460 nm emission peak occurs with the increase of temperature. Of course, the underlying mechanisms may be complex and require further study.

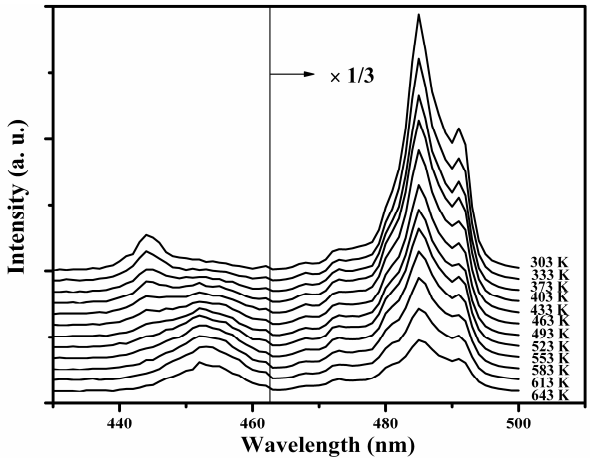

Fig. 7. Temperature dependent blue upconversion emissions in Ho^{3+}/Yb^{3+} codoped glass ceramic.

The change in the intensity ratio between the two blue emissions is originated from the small energy gap between the $^5F_{2,3}/^3K_8$ and $^5F_1/^5G_6$ levels, which allows the ions on the $^5F_{2,3}/^3K_8$ to be thermally populated onto the $^5F_1/^5G_6$ levels. It has been well known that the relative population of the thermally coupled levels follows a Boltzman type population distribution, and according to the theory by Wade et al. [19], the FIR for the emissions from the thermally coupled levels of RE ions is modified as

$$FIR \equiv \frac{I_i}{I_j} = \frac{A_i g_i \sigma_i w_i}{A_j g_j \sigma_j w_j} \exp\left(-\frac{\Delta E}{k_B T}\right) + B = C \exp\left(-\frac{\Delta E}{k_B T}\right) + B, \qquad (6)$$

where I, A, and g are the fluorescence intensity, spontaneous emission rate, degeneracy for transitions from the upper (i) and the lower (j) thermally coupled levels, respectively; σ is the response of the detection system to the emission with angular frequency w; the pre-exponential parameter is defined as $C = A_i g_i \sigma_i w_i / A_j g_j \sigma_j w_j$; B is a constant defined as the offset factor. Figure 8 presents the FIR between the shorter and the longer wavelength blue emissions from Ho^{3+}/Yb^{3+} codoped glass ceramic as a function of temperature. The experimental data are fitted by Eq. (6). It can be observed that the fittings agree well with the experimental data. C and B are fitted to be about 4.22 ± 0.73 and 0.043 ± 0.002, respectively, and ΔE is fitted to be about 1544.6 ± 81 cm^{-1}. Several temperature circles have been tested and a good repeatability was obtained. In addition, to understand whether the heating effect generated by the absorption of Yb^{3+} ions at 980 nm influences the quasi-thermal equilibrium of the sample, the temperature dependent ratios were recorded when the sample was excited with a lower power of 330 mW. The result illustrates that the ratios can also be well fitted by the Boltzman distribution of Eq. (1) with slight change in the values of the fitted parameters,

#168888 - $15.00 USD Received 22 May 2012; revised 4 Jul 2012; accepted 4 Jul 2012; published 23 Jul 2012

indicating the quasi-thermal equilibrium condition of the sample is hardly affected by pump absorption heating. And based on the above experiment results, such heating effect on the optical thermometry actually can be eliminated by the offset factor B in Eq. (1). Table 1 shows the expression of the sensitivity for Ho^{3+}/Yb^{3+} codoped glass ceramic. For comparison, the sensitivities for the other RE ions doped materials are also presented. It is observed that optical temperature sensors with excellent sensitivity can be realized by using Ho^{3+}/Yb^{3+} codoped glass ceramic. This result is attributed to the large energy gap between $^5F_{2,3}/^3K_8$ and $^5F_1/^5G_6$ states, which is also in favor of a high resolution.

For optical temperature sensors, it is also necessary to know the variation of sensitivity with temperature. Then, the relative sensitivity S_R has been defined as [28, 29]

$$S_R \equiv \frac{dFIR}{dT} = FIR \times \frac{\Delta E}{k_B T^2}. \tag{7}$$

The experimental and theoretically calculated results of S_R for our sample are shown in Fig. 9. The S_R keeps increasing with temperature and can be expected to reach its theoretical maximum value (about 1.02×10^{-3} K^{-1}) at 1119 K. For comparison, the theoretical maximum value $S_{R\text{-}MAX}$ and their corresponding temperatures for other temperature sensors in the literature [20, 28–30] are also shown in Table 1. From the table, one can conclude that Ho^{3+} ions are appropriate to be used as the activators for high temperature measurements.

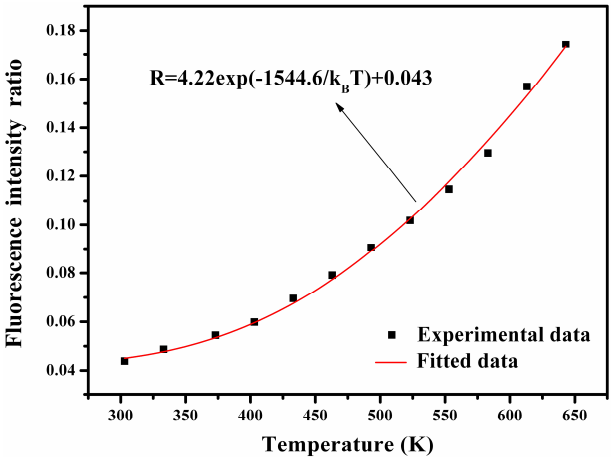

Fig. 8. Fluorescence intensity ratio between the blue emissions from Ho^{3+}/Yb^{3+} codoped glass ceramic as a function of temperature.

Table 1. The Absolute Sensitivities S_A and the Theoretical Maximum Value of the Relative Sensitivity $S_{R\text{-}MAX}$ as well as the Temperature T for $S_{R\text{-}MAX}$ in Optical Temperature Sensors Based on the Fluorescence of Materials with Rare Earth Ions.

Rare earth (Materials)	Transitions	$S_A(K^{-1})$	Temperature range (K)	$S_{R\text{-}MAX}$ ($\times 10^{-3}K^{-1}$)	T (K)	Reference
Ho^{3+} (glass ceramic)	$^5F_{2,3}/^3K_8$, $^5F_1/^5G_6 \rightarrow {}^5I_8$	$2238.6/T^2$	303-643	1.02	1119	This work
Er^{3+} (chalcogenide glass)	$^2H_{11/2}$, $^4S_{3/2} \rightarrow {}^4I_{15/2}$	$928.9/T^2$	293-528	5.21	464	Ref [28].
Pr^{3+} (tellurite glass)	$^3P_1, ^3P_0 \rightarrow {}^3H_4$	$880.5/T^2$	273-453	16.32	440	Ref [30].
Yb^{3+} (silica)	$^2F_{5/2(a)}$, $^2F_{5/2(b)} \rightarrow {}^2F_{7/2}$	$1305.8/T^2$	297-433	0.09	653	Ref [20].
Nd^{3+} (glass ceramic)	$^4F_{5/2}$, $^4F_{3/2} \rightarrow {}^4I_{9/2}$	$1371.5/T^2$	300-700	1.50	600	Ref [29].

#168888 - $15.00 USD Received 22 May 2012; revised 4 Jul 2012; accepted 4 Jul 2012; published 23 Jul 2012

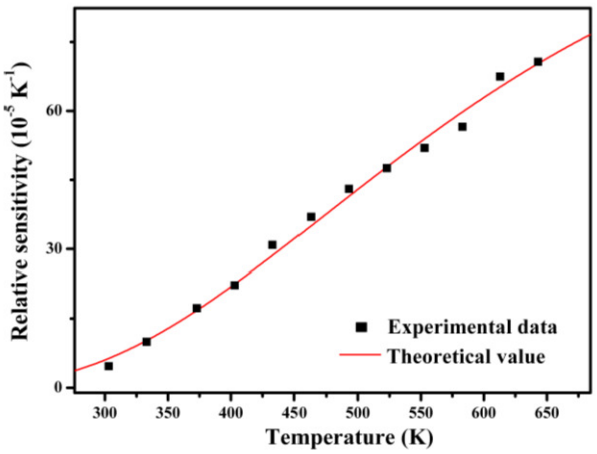

Fig. 9. Relative sensitivity of Ho^{3+}/Yb^{3+}codoped glass ceramic for optical thermometry as a function of temperature.

4. Conclusion

In conclusion, Ho^{3+}/Yb^{3+} codoped glass ceramic was prepared. Under 980 nm excitation, the short-wavelength UC emissions in the spectral range of ultraviolet-blue were successfully obtained. The luminescence decay curves were measured, and it was found that the weakened multiphonon nonradiative relaxations and the enhanced energy transfer from Yb^{3+} to Ho^{3+} in the glass ceramic played an important role in such phenomenon. Furthermore, the thermal behavior of the blue emissions from Ho^{3+}/Yb^{3+} codoped glass ceramic at temperatures ranging from 303 to 643 K was investigated. It was observed that by using the FIR technique, appreciable sensitivity for temperature measurement can be achieved by using the Ho^{3+}/Yb^{3+} codoped glass ceramic as the sensing medium This result suggests that the Ho^{3+}/Yb^{3+} codoped glass ceramic is a good medium for optical temperature sensors with high sensitivity, high resolution as well as good accuracy.

#168888 - $15.00 USD Received 22 May 2012; revised 4 Jul 2012; accepted 4 Jul 2012; published 23 Jul 2012